NIH Public Access
Author Manuscript
Clin Neurophysiol. Author manuscript; available in PMC 2015 June 01.

Published in final edited form as:
Clin Neurophysiol. 2014 June ; 125(6): 1202–1212. doi:10.1016/j.clinph.2013.11.038.

Coil Design Considerations for Deep Transcranial Magnetic Stimulation

Zhi-De Deng[a,b], **Sarah H. Lisanby**[a,c], and **Angel V. Peterchev**[a,d,e,*]

[a]Department of Psychiatry and Behavioral Sciences, Duke University, Durham, NC, USA

[b]Department of Electrical Engineering, Columbia University, New York NY, USA

[c]Department of Psychology and Neuroscience, Duke University, Durham, NC, USA

[d]Department of Biomedical Engineering, Duke University, Durham, NC, USA

[e]Department of Electrical and Computer Engineering, Duke University, Durham, NC, USA

Abstract

Objectives—To explore the field characteristics and design tradeoffs of coils for deep transcranial magnetic stimulation (dTMS).

Methods—We simulated parametrically two dTMS coil designs on a spherical head model using the finite element method, and compare them with five commercial TMS coils, including two that are FDA approved for the treatment of depression (ferromagnetic-core figure-8 and H1 coil).

Results—Smaller coils have a focality advantage over larger coils; however, this advantage diminishes with increasing target depth. Smaller coils have the disadvantage of producing stronger field in the superficial cortex and requiring more energy. When the coil dimensions are large relative to the head size, the electric field decay in depth becomes linear, indicating that, at best, the electric field attenuation is directly proportional to the depth of the target. Ferromagnetic cores improve electrical efficiency for targeting superficial brain areas; however magnetic saturation reduces the effectiveness of the core for deeper targets, especially for highly focal coils. Distancing winding segments from the head, as in the H1 coil, increases the required stimulation energy.

Conclusions—Among standard commercial coils, the double cone coil offers high energy efficiency and balance between stimulated volume and superficial field strength. Direct TMS of targets at depths of ~ 4 cm or more results in superficial stimulation strength that exceeds the upper limit in current rTMS safety guidelines. Approaching depths of ~ 6 cm is almost certainly unsafe considering the excessive superficial stimulation strength and activated brain volume.

© 2013 International Federation of Clinical Neurophysiology. Published by Elsevier Ireland Ltd. All rights reserved.

*Corresponding author. Tel: +1 919 684 0383; fax: +1 919 681 9962. angel.peterchev@duke.edu.

Publisher's Disclaimer: This is a PDF file of an unedited manuscript that has been accepted for publication. As a service to our customers we are providing this early version of the manuscript. The manuscript will undergo copyediting, typesetting, and review of the resulting proof before it is published in its final citable form. Please note that during the production process errors may be discovered which could affect the content, and all legal disclaimers that apply to the journal pertain.

NIH-PA Author Manuscript

NIH-PA Author Manuscript

NIH-PA Author Manuscript

NIH-PA Author Manuscript

NIH-PA Author Manuscript

NIH-PA Author Manuscript

Significance—Coil design limitations and tradeoffs are important for rational and safe exploration of dTMS.

Keywords

Deep transcranial magnetic stimulation; Electric field; Focality; Energy; Model

1. Introduction

Transcranial magnetic stimulation (TMS) uses brief, strong magnetic pulses to induce an electric field in the brain that modulates neural activity. Repetitive TMS (rTMS) can produce changes in neural activity that persist beyond the period of stimulation. Therefore, rTMS can be used as a probe of higher brain functions and an intervention for psychiatric and neurological disorders (Fitzgerald et al., 2006; Fitzgerald and Daskalakis, 2011).

Due to the rapid attenuation in depth of the electric field of conventional stimulation coils, TMS has been restricted to superficial cortical targets, typically 2–3 cm in depth. For example, the most common target in TMS depression treatments is superficial—the dorsolateral prefrontal cortex (Fitzgerald and Daskalakis, 2011). However, alternative stimulation targets for depression may include non-superficial (~3–5 cm depth) brain areas such as frontopolar, medial frontal, and orbitofrontal cortices (Downar and Daskalakis, 2013; Seminowicz et al., 2004; Johansen-Berg et al., 2008), as well as deeper (~6–8 cm depth) brain areas such as subcallosal cingulate cortex (Mayberg et al., 2005; Lozano et al., 2008; Kennedy et al., 2011; Holtzheimer et al., 2012), the ventral portion of the anterior limb of the internal capsule and adjacent dorsal ventral striatum (Greenberg et al., 2005; Malone et al., 2009), nucleus accumbens (Roth and Zangen, 2006; Schlaepfer et al., 2008; Bewernick et al., 2010), amygdala (Roth and Zangen, 2006), inferior thalamic peduncle (Jiménez et al., 2005), and lateral habenula (Sartorius and Henn, 2007; Sartorius et al., 2010).

While accessing such deep brain therapeutic targets directly with deep TMS (dTMS) is compelling, the induction of deeply penetrating electric field has fundamental physical limitations. It has been theoretically proven that inside a spherically symmetric volume conductor, it is impossible for any TMS coil configuration to produce three-dimensional focusing of the electric field in depth (Heller and van Hulsteyn, 1992). The induced electric field is always strongest on the surface of a uniform conductor and drops off in depth. Further, in a uniformly conducting sphere or spherical shells, the radial electric field component is always zero; hence, the electric field at the center of the sphere is zero (Roth et al., 1990; Eaton, 1992; Cohen and Cuffin, 1991; Ruohonen and Ilmoniemi, 2002). The non-spherical shape of a real head and the presence of tissue anisotropy and non-tangential boundaries can create local maxima of the electric field in depth (Thielscher et al., 2011; Davey et al., 2003; Miranda et al., 2003, 2007; Opitz et al., 2011). However, local electric field maxima created by the brain anatomy only partially compensate for the stronger driving electric field in more superficial regions. Furthermore, brain anatomy varies among individuals and hence is difficult to account for in coil design. Finally, the electric field of larger coils decays slower in depth but is intrinsically less focal, and figure-8 type coils are

NIH-PA Author Manuscript

NIH-PA Author Manuscript

NIH-PA Author Manuscript

fundamentally more focal than circular type coils (Ruohonen and Ilmoniemi, 2002; Ueno et al., 1988; Rösler et al., 1989; Grandori and Ravazzani, 1991; Deng et al., 2013).

Within these fundamental limitations, a number of dTMS coil designs have been investigated or proposed. The double cone coil—formed by two adjacent, 110 mm diameter, circular windings fixed at a 100° angle—induces a more deeply penetrating and less focal electric field compared to a planar, 70 mm winding diameter figure-8 coil (Deng et al., 2013; Lontis et al., 2006). The double cone coil has been used for direct activation of the pelvic floor and lower limb motor representation at the interhemispheric fissure (Terao et al., 1994) as well as for transsynaptic activation of the anterior cingulate cortex via stimulation of the medial frontal cortex (Hayward et al., 2007). Double cone type coils are also highly efficient for seizure induction (Lisanby et al., 2001, 2003; Deng et al., 2011; Kayser et al., 2011). This is an advantage in the context of magnetic seizure therapy, but in subconvulsive applications, this is a significant source of risk.

A family of dTMS coil designs called Hesed (H) coils has been developed with the goal of effective stimulation of deep brain structures (Roth et al., 2002; Zangen et al., 2005; Roth et al., 2007a,b). More than twenty different types of H coils have been designed and manufactured for various applications (Roth et al., 2013). H coils typically have complex winding patterns and larger dimensions compared to conventional coils and consequently have slower electric field attenuation with depth, at the expense of reduced focality (Deng et al., 2013). It has been proposed that the electric efficiency, field depth, and focality of H coils can be improved by the use of high-permeability ferromagnetic cores, but the reported improvements were minor (Salvador et al., 2009; Deng et al., 2013). H coils have been evaluated for the treatment of a variety of psychiatric and neurological disorders (Bersani et al., 2013), including major depression (Levkovitz et al., 2007, 2009; Rosenberg et al., 2010a,b; Harel et al., 2011; Rosenberg et al., 2011a; Isserles et al., 2011; Levkovitz et al., 2011b; Harel et al., 2012; Bersani et al., 2012), schizophrenia (Levkovitz et al., 2011a; Rosenberg et al., 2011b), dystonia (Kranz et al., 2010), autism (Enticott et al., 2011; Krause et al., 2012), pain (Tartaglia et al., 2011), chronic migraine (Dalla Libera et al., 2011), post-traumatic stress disorder (Isserles et al., 2013), and logopenic primary progressive aphasia (Trebbastoni et al., 2012). An rTMS system using the H1 coil received clearance by the U. S. Food and Drug Administration (FDA) for the treatment of depression.

Other dTMS strategies have been proposed as well. Based on analysis and simulations, it was suggested that a C-shaped ferromagnetic core coil with a wide opening angle (Figure 1(b)) can suppress the surface field and, consequently, could reduce scalp stimulation (Davey, 2008; Davey and Riehl, 2006; Al-Mutawaly et al., 2001). It is unclear whether the addition of ferromagnetic cores is practical as they might enter magnetic saturation in the field range needed for dTMS. In addition to the C-core coil, large circular type dTMS coils have been proposed, including the crown coil (Figure 1(a)) (Deng et al., 2008) and the halo coil (Ishii et al., 2008; Crowther et al., 2011). The effects of low-field magnetic stimulation with large MRI gradient coils have also been investigated (Rohan et al., 2004; Carlezon et al., 2005; Volkow et al., 2010; Deng et al., 2013).

NIH-PA Author Manuscript

NIH-PA Author Manuscript

NIH-PA Author Manuscript

Temporal summation at the neural membrane has also been proposed for enabling focused stimulation of deep brain regions via sequential firing of TMS pulses from a set of coil windings positioned around the head, with no activation of cortical brain regions (Roth et al., 2007b). Preliminary theoretical analysis, however, indicates that sequential firing of coil windings produces less neural membrane depolarization than conventional synchronous firing of all windings, suggesting that this strategy for enhancing stimulation in depth may be ineffective (Deng et al., 2008).

All of these dTMS approaches use coils that have larger dimensions than conventional superficial TMS coils, and consequently provide slower decay rate of the electric field with distance, at the expense of reduced intrinsic focality (Deng et al., 2013). Compared to large coils, smaller coils induce an electric field that is intrinsically more focal; however, the improvement in focality is accompanied by faster field attenuation in depth (Deng et al., 2013). Therefore, in order to achieve the same electric field strength at a target depth, smaller coils would require higher coil current to compensate for the faster field drop-off. Higher coil current, in turn, could lead to larger activated brain volume, which counteracts the gain in intrinsic focality of smaller coils. Therefore, it is important to characterize how the field attenuation in depth affects the activated brain volume for different coil sizes. These results can inform dTMS coil selection for various stimulation target depths. Finally, dTMS requires higher energy than superficial TMS, but the energy requirements of various dTMS coil designs have not been systematically compared.

The present study extends our previous work (Deng et al., 2013) to systematically explore the effect of coil configuration and size on the stimulation strength, focality, and energy for deep brain targets. We evaluate the electric field characteristics and pulse energy when the coil current is adjusted to produce threshold electric field strength at various depths in the brain. In addition, we explore the practicality of incorporating ferromagnetic cores in dTMS coils to reduce stimulation energy. This analysis includes models of the coils from the two commercial rTMS systems approved by the FDA for therapeutic applications (treatment of depression).

This study has been presented in part in a conference proceeding (Deng et al., 2008).

2. Materials and methods

The head, coils, and electric field were modeled with the electromagnetic finite element package MagNet (Infolytica, Inc., Canada). Post-processing was carried out in MagNet and in MATLAB (The MathWorks, Natick, MA, USA). The electric field simulation methods are described in detail and validated experimentally in our previous study (Deng et al., 2011).

2.1. Head model

The human head was modeled as a homogeneous sphere with radius of 8.5 cm and isotropic conductivity of 0.33 S m^{-1}. The distinct head tissue layers (scalp, skull, corticospinal fluid, and brain) were not differentiated since magnetically induced electric field in a sphere is insensitive to radial variations of conductivity (Eaton, 1992). The cortical surface and the

NIH-PA Author Manuscript

NIH-PA Author Manuscript

NIH-PA Author Manuscript

gray matter–white matter interface were assumed to be at depths of 1.5 cm and 2 cm from the surface of the head, respectively (Epstein et al., 1990).

Even though the spherical model substantially simplifies the head geometry, it is a practical reduction for parametric studies that focus on the electric field characteristics of TMS coils rather than on specific anatomical targets in the brain (Eaton, 1992; Cohen and Cuffin, 1991; Ruohonen and Ilmoniemi, 2002; Grandori and Ravazzani, 1991; Ravazzani et al., 1996; Saypol et al., 1991; Roth et al., 1991; Deng et al., 2011, 2013). Unlike individualized realistic head models (e.g. see (Opitz et al., 2011)), results obtained with the spherical model or other head models of intermediate complexity (e.g. see (Wagner et al., 2004)) are not limited to a particular subject's head anatomy and coil position, allowing general conclusions about the effect of coil characteristics and stimulation intensity. Furthermore, the spherical model provides a standardized platform for evaluating coil designs that can be replicated easily by various researchers.

2.2. Coil models

We study the tradeoffs among electric field characteristics in two ways. First, we analyze two parameterized coil designs (crown and C-core, shown in Figure 1(a–b)), to demonstrate the dependence of the electric field and energy on coil size, while eliminating the confound of different coil topologies. Then, we compare fixed coil designs, which include representative crown and C-core coils as well as commercial coils with varying sizes and shapes (Figure 2), to show that the parametric findings are valid across topologies and to link the simulation results to clinical studies.

In the parameterized crown and C-core coils, the number of winding turns was kept fixed within coil type since under this condition only spatial factors affect the performance metrics. The number of turns for the crown and C-core coil types was selected to produce inductance in the range of conventional TMS coils. The minimum spacing between the coil windings and the surface of the head model was 5 mm to account for the thickness of the coil insulation. Ferromagnetic cores were modeled with a linear, homogeneous, isotropic material with relative permeability of 1000 and conductivity of 1 S m^{-1} (Salvador et al., 2007, 2009; Davey, 2008). Thus, we did not explicitly model core saturation. Separately, we estimated the degree of core saturation that would occur for a specific coil current by calculating the percentage of the core volume that has flux density above the saturation flux density. We evaluated silicon steel and vanadium permendur as representative core materials with saturation flux density of 1.8 T and 2.3 T, respectively. The linear material approximation does not account for the fact that core saturation would reduce the electric field strength (due to increased magnetic reluctance) and pulse duration (due to decreased inductance); nevertheless, this approach provides insight into the scale of the saturation problem.

2.2.1. Crown coil—The crown coil is a large circular coil wound around the perimeter of the head like a crown. A simplified model of the crown coil is shown in Figure 1(a). The distance from the vertex to the mid-latitude of the coil is parameterized by angle α and the spread of the winding is parameterized by angle β. The number of winding turns was fixed

NIH-PA Author Manuscript

NIH-PA Author Manuscript

NIH-PA Author Manuscript

at 9. In an actual implementation (Figure 2(c)), the anterior portion of the winding could lie, for example, over the forehead so that the induced electric field could stimulate the frontopolar, medial frontal, and orbitofrontal cortices.

2.2.2. C-core coil—A cutaway view of a C-core coil (Davey and Riehl, 2006) is shown in Figure 1(b). The coil is wound around a stretched C-shaped ferromagnetic core with arc-opening angle γ. The core has a rectangular cross section with height *h* and width *w*; both are fixed at 7 cm in this study. The number of turns was fixed at 10. A C-core coil implementation with discrete winding turns is shown in Figure 2(g).

2.2.3. Commercial coils—In addition to the crown and C-core coils, we modeled five commercial TMS coil configurations, including the Magstim (Whitland, Wales, UK) 90 mm circular coil (P/N 3192, Figure 2(a)); Brainsway (Jerusalem, Israel) H1 coil (Figure 2(b)); Magstim 70 mm figure-8 coil (P/N 9225 and P/N 3190, figure 2(d)); Neuronetics (Malvern, PA, USA) ferromagnetic core figure-8 coil (P/N CRS 2100, Figure 2(e)); and Magstim double cone coil (P/N 9902, Figure 2(f)). The Brainsway H1 coil (Figure 2(b)) and the Neuronetics ferromagnetic core figure-8 coil (Figure 2(e)) belong to rTMS systems that are approved by the FDA for the treatment of depression.

2.3. Electric field computation

The spatial electric field distribution was computed with the 3-D time-harmonic solver of MagNet using an arbitrary coil current $I_0 = 1$ A and angular frequency $\omega_0 = 2\pi \times 5$ kHz which is representative of efficient TMS pulses (Davey et al., 2003; Davey and Riehl, 2006). Since the head tissues are non-magnetic and the quasistatic approximation is applicable in the frequency range of TMS pulses (< 10 kHz) (Thielscher et al., 2011; Plonsey and Heppner, 1967; Logothetis et al., 2007), tissue permeability and permittivity were set to those of free space. Furthermore, the value of the low-frequency tissue conductivity has no effect on the distribution of the induced electric field in the spherical head model (Eaton, 1992; Davey et al., 2003). MagNet solves for the magnetic field via the edge-element version of the T-Ω method. The electric field is computed from the magnetic field using Ampère's and Ohm's Laws. The electric field was scaled to account for the peak rate of change of the coil current (Deng et al., 2011). The peak rate of change of the coil current is linearly proportional to the capacitor voltage, which is adjusted to produce the desired electric field strength at various target depths.

2.4. Coil performance metrics

In our previous analysis of 50 TMS coils (Deng et al., 2013), we introduced metrics for characterizing the induced electric field spatial distribution that are normalized to the superficial field magnitude (tangential spread and depth of penetration) and are therefore independent of the device output and the neuronal response threshold. In the present analysis for dTMS coil design, we consider coil performance metrics involving electric field normalization to threshold strength at various target depths since, unlike conventional TMS, dTMS targets are not superficial. The electric field threshold for neuronal activation depends on the stimulus waveform temporal characteristics, which are in turn affected by factors such as the coil inductance, energy-storage capacitance, and circuit resistance (Deng et al.,

NIH-PA Author Manuscript

NIH-PA Author Manuscript

NIH-PA Author Manuscript

2011; Peterchev et al., 2012). Therefore, we assume that the electric field waveform shape and pulse width for all coils are matched in order to produce an identical neural activation threshold, E_{th}. To keep the pulse width fixed in the presence of various coil inductance values, we assumed that the stimulator capacitance is adjusted so that the inductance × capacitance product is constant, or that a TMS device producing rectangular pulses with controllable pulse width is used (Peterchev et al., 2008, 2011). We use metrics to quantify the stimulation strength and focality that are independent of the specific value of E_{th} (see sections 2.4.1 and 2.4.2). For the calculation of the absolute stimulation energy (sections 2.4.3) we assume E_{th} = 1 V cm^{-1} (Epstein et al., 1990; Rudiak and Marg, 1994; Thielscher and Kammer, 2002; Kammer et al., 2001; Davey and Riehl, 2006).

2.4.1. Electric field strength in superficial cortex—We quantified the peak electric field strength in the superficial cortex relative to neural activation threshold, $\max(|E_{2\ cm}|)/E_{th}$, when the induced electric field magnitude at the target depth d, $|E_d|$, is at the neural activation threshold, E_{th}.

2.4.2. Electric field focality—We quantified the neural activation focality, V_A, by the percentage of the brain sphere exposed to suprathreshold electric field (Deng et al., 2011). Assuming that the peak electric field strength at a target depth, $|E_d|$, is at threshold, then V_A equals the ratio between the brain volume where $|E| \geq |E_d|$ and the total brain volume (1,437 cm^3).

2.4.3. Coil energy—The energy delivered to the coil, W, was calculated by integrating $\mathbf{B} \cdot \mathbf{H}$ over space

$$W = \frac{1}{2}\int\int\int \mathbf{B}\cdot\mathbf{H}\mathrm{d}^3x \quad (1)$$

where **B** and **H** are the magnetic flux density and magnetic field intensity, respectively (Jackson, 1999). The energy required to achieve threshold electric field at a target depth d is obtained by scaling W for an arbitrary current by $(E_{th}/|E_d|)^2$, where E_{th} = 1 V cm^{-1}.

3. Results

3.1. Effect of coil size

3.1.1. Electric field penetration limit—Figure 1(c) and (d) shows the electric field attenuation in depth for various sizes of the crown and C-core coils, respectively. Illustrated in Figure 1(c), as angle α controlling the radius of the crown coil increases, the electric field attenuation becomes progressively more linear. Similarly, increasing the crown coil opening angle β reduces the rate of electric field attenuation. Indeed, for α = 90°, in the limit as β approaches 180° the crown coil converges to a flux ball where the magnetic field intensity in the head is uniform (Haus and Melcher, 1989; Jackson, 1999), resulting in electric field attenuation in depth that is linear. Though the flux ball configuration is not physically realizable for brain stimulation, it illustrates the limiting case of linear electric field attenuation. Similarly, shown in Figure 1(d), as angle γ of the C-core coil increases to 180°, the rate of electric field attenuation decreases and approaches linear decay.

NIH-PA Author Manuscript

NIH-PA Author Manuscript

NIH-PA Author Manuscript

The observation that the electric field decay becomes linear for large coil size allows us to calculate a fundamental limit for field penetration. Namely, the ratio of the local electric field maxima at two depths, d_1 and d_2, is

$$\frac{\max(|E_{d_1}|)}{\max(|E_2|)} = \frac{R - d_1}{R - d_2} \quad (2)$$

where R is the head radius. For example, according to (2), for very large coils, regardless of coil configuration, the ratio of the field strength at 4 cm depth to that in the cortex is $\frac{\max(|E_{4\mathrm{cm}}|)}{\max(|E_{2\mathrm{cm}}|)} = 0.69$, deteriorating to $\frac{\max(|E_{6\mathrm{cm}}|)}{\max(|E_{2\mathrm{cm}}|)} = 0.38$ for 6 cm target depth. Further, in this limiting case for large coils, the ratio of the field strength in the scalp to that in the cortex is $\frac{\max(|E_{0.25\mathrm{cm}}|)}{\max(|E_{2\mathrm{cm}}|)} = 1.27$.

Equation (2) can also be used to estimate the maximum possible depth of direct neural activation when stimulation is applied at a given strength relative to motor threshold, as is conventional in many TMS applications. For this analysis we assume that the target area for conventional motor threshold determination is at about 2 cm depth, d_1 = 2 cm (Epstein et al., 1990; Rudiak and Marg, 1994). For target depth d_2, the ratio $\frac{\max(|E_{2\mathrm{cm}}|)}{\max(|E_{d_2}|)}$ represents the factor by which the stimulation strength at 2 cm depth exceeds the motor threshold. The resulting maximum direct stimulation depth versus stimulation strength relative to motor threshold is plotted in Figure 3. For example, at 120% motor threshold, which is commonly used for dosing of therapeutic rTMS protocols (Johnson et al., 2013; Levkovitz et al., 2009), the maximum stimulation depth is d_2 = 3.08 cm. Thus, when dosed at 120% motor threshold, even relatively large coils used for dTMS would stimulate not much deeper than ~ 3 cm. Further, to reach depth of 4 cm, the superficial cortical strength would be 145% of motor threshold, which exceeds the range of intensities covered in the current rTMS safety guidelines (≤ 130% motor threshold) (Rossi et al., 2009).

3.1.2. Stimulation strength, volume, and energy—The performance metrics defined in section 2.4 were computed for the crown coil and the C-core coil and plotted in Figure 4 as a function of angles α (for β = 40°) and γ (for $h = w$ = 7 cm). The maximum electric field strength in the cortex relative to neural activation threshold, $\max(|E_{2\ \mathrm{cm}}|)/E_{\mathrm{th}}$, activated brain volume, V_{A}, and coil energy, W, were calculated for electric field strength of 1 V cm^{-1} at depths of 4 cm and 6 cm. For a fixed electric field strength in depth, increasing the coil size reduces the field strength in the superficial cortex (Figure 4(a–b)), at the expense of stimulating a broader brain volume (Figure 4(c–d)). As coil size increases, the energy initially decreases and then plateaus (Figure 4(e–f)), suggesting that the gain in energy efficiency diminishes for larger coils. Figure 4 indicates that the stimulation strength in cortex, volume, and energy all increase with stimulation target depth (6 cm versus 4 cm).

Figure 5 shows that the rate of increase of the performance metrics with depth is affected by coil size. To examine the relative effect of coil size, in Figure 5 the performance metrics are normalized to those for the nominal crown and C-core coil designs displayed in Figure 2(c)

NIH-PA Author Manuscript

NIH-PA Author Manuscript

NIH-PA Author Manuscript

and (g), respectively. Figure 5(a–b) demonstrates that the normalized cortical field strength $|E_{2\ cm}|$ deviates farther from unity as the stimulation target depth increases, indicating that the difference in cortical field strength between large and small coils increases with depth. This behavior is a direct consequence of the faster electric field decay in depth of smaller coils compared to larger coils.

Figure 5(c–d) shows that the normalized activated volume V_A converges toward unity as the stimulation target depth increases. This implies that smaller coils retain a focality advantage over larger coils, but this advantage diminishes with stimulation depth. For very large C-core coils, $V_A/V_{A,\ \gamma=140}$ initially rises for superficial stimulation target depths (Figure 5(d)). This is possibly due to the fact that when the opening angle increases, the field maximum on the surface under the center of the coil spreads outward along the length of the coil, increasing the normalized activated volume for superficial stimulation target depths.

Compared to smaller crown coils, larger crown coils are more energy efficient for all stimulation target depths, as shown in Figure 5(e). The large-coil energy advantage grows with stimulation depth, as the normalized W diverges with increasing stimulation depth. On the other hand, Figure 5(f) indicates that for the C-core coils there is an optimal coil size that results in minimum energy requirement for each target depth. The energy-optimal C-core angle $\gamma_{optimal}$ is increasing approximately linearly with target depth (see Supplementary Figure S2). The nominal $\gamma = 140°$ C-core coil, for example, is the most energy efficient configuration for stimulating targets at approximately 4.5 cm in depth.

3.2. Comparison of coil configurations

Figure 2 depicts five commercial TMS coils and representative crown and C-core coil designs with their corresponding electric field distributions. Based on the electric field distribution, the coils can be divided into two groups (Deng et al., 2013). The first group of coils, which includes the 90 mm circular, H1, and crown coil, induces a single circular or near circular loop of eddy current (Figure 2(a–c)). When centered near vertex, the first group of coils induces a circular electric field in the transverse plane of the head and a nonfocal ring-shaped electric field maximum under the coil perimeter. The second group of coils, which includes the figure-8, double cone, and C-core coils, induces two symmetric loops of eddy current with a single electric field maximum under the center of the coil (Figure 2(d–g)). Thus, compared to circular type coils, the figure-8 type coils are more focal.

Figure 6 compares performance metrics for the coils from Figure 2. Figure 6(a–c) shows, respectively, the peak electric field in the superficial cortex, $\max(|E_{2\ cm}|)$, directly activated brain volume, V_A, and coil energy, W, required to induce 1 V cm^{-1} field strength at target depths of 2–6 cm. For all coils these metrics increase with deeper stimulation targets, consistent with Figure 4, but the rate of increase and offset of the curves depend on the specific coil design. Smaller coils have higher rate of increase of the superficial cortex field strength with increasing target depth (Figure 6(a)) since these coils exhibit faster field attenuation in depth. The figure-8 type coils (black curves) generally activate smaller brain volume than circular type coils (red curves), although the C-core coil's V_A is comparable or larger than that of circular coils for target depths beyond 4 cm (Figure 6(b)).

NIH-PA Author Manuscript

NIH-PA Author Manuscript

NIH-PA Author Manuscript

The data in Figure 6 confirm the observation of a tradeoff between superficial electric field strength and stimulated volume as a function of coil size. Nevertheless, for all coils, $|E_{2\ cm}|/E_{th} > 3$ (corresponding to superficial stimulation at 300% motor threshold) and $V_A >$ 40% for target depths ≥ 6 cm, indicating massive direct stimulation of the brain. Finally, the relative differences in V_A among the coils decrease for deeper targets, indicating that the focality advantage of smaller coils is diminished in depth, consistent with the parametric analysis in Figure 5(c–d).

Figure 6(c) indicates that the crown coil is the most energy efficient for stimulating deep brain structures, whereas the air core figure-8 coil is the least efficient. The double cone coil is the second most efficient, likely because of the relatively large winding loop size and the tight coupling to the head. The H1 coil is the second least efficient, likely a consequence of the perpendicular winding segments that create magnetic flux in the air not coupled to the head. The C-core and crown coils show the slowest rate of increase of the energy with increasing target depth, because of their slow electric field attenuation in depth. Consistent with results in the literature (Epstein and Davey, 2002; Davey and Epstein, 2000; Peterchev et al., 2011), the ferromagnetic core reduces the required energy for the figure-8 coil more than three times.

The ferromagnetic cores of the figure-8 and C-core coils may enter saturation when the current strength is increased to stimulate deep targets. The percentage of the core in saturation increases with increasing target depth (see Supplementary Figure S3). For a given target depth, core saturation is more significant in focal coils, such as the standard-size figure-8 coil, compared to less focal coils, such as the C-core coil. For example, at the current strength nominally required to reach a 4 cm deep target, the vanadium permendur cores of the figure-8 and C-core coils would be 37% and 5% saturated, respectively. To reach a 6 cm deep target, the cores would be saturated over 84% for both core materials.

4. Discussion

4.1. Stimulation strength, depth, and focality tradeoffs

For a given target depth, there is a tradeoff between the superficial electric field strength and focality that depends on the coil size. Larger coils have an electric field that decays slower in depth (Figure 1(c–d)) but is less focal (Figure 4(c–d)) than that of smaller coils. Consequently, to stimulate deep targets, large coils generate an electric field that is weaker in the superficial cortex (Figure 4(a–b), Figure 6(a)) but that stimulates a larger volume of the brain (Figure 4(c–d), Figure 6(b)) compared to smaller coils.

Although smaller coils are intrinsically more focal than larger coil (Deng et al., 2013), the focality advantage in terms of activated brain volume diminishes with increasing target depth (see Figure 5(c–d)). This is a result of the faster electric field attenuation in depth for small coils which necessitates a larger increase of the coil current to reach a specific deep target compared to large coils. The faster increase of the required current with target depth results in a faster increase of the activated brain volume for small coils.

NIH-PA Author Manuscript

NIH-PA Author Manuscript

NIH-PA Author Manuscript

4.2. Safety and tolerability

The tradeoffs among stimulation strength, depth, and focality raise the question of what is a more tolerable, safe, and effective approach to dTMS—to stimulate a smaller brain volume (and scalp surface) at a higher intensity relative to threshold, or to stimulate a larger brain volume (and scalp surface) at an intensity closer to, but still higher than, threshold.

As shown in Figures 4(a–c) and Figures 6(a), for the examined dTMS coils the worst case peak electric field in the brain is below 9 V cm^{-1}, assuming E_{th} = 1 V cm^{-1}, which is less than two times the peak electric field of 5.4 V cm^{-1} generated by a conventional figure-8 coil and TMS device at peak output (Hovey and Jalinous, 2006). Therefore, safety metrics such as induced charge density and temperature increase are still well below the recommended limits for tissue damage (Agnew and McCreery, 1987; Ruohonen and Ilmoniemi, 2002; Hovey and Jalinous, 2006; Rossi et al., 2009; IEEE Std C95.1-2005, 2005; International Commission on Non-Ionizing Radiation Protection, 2010). Therefore, undesirable stimulation and neuromodulation in non-target brain regions and risk of seizure induction are more relevant safety concerns than the risk of tissue damage. For example, large circular type coils like the crown coil and the H1 coil may stimulate frontal, lateral, and posterior brain regions to a comparable degree because of the approximately circular current flow in the transverse plane of the head (see Figure 2(a–c)). Focusing of the electric field in frontal regions could be improved to some degree by spreading out or distancing from the head the windings toward the posterior, as illustrated by the H1 coil and variants of the crown coil (Deng et al., 2013). The effectiveness of this approach, however, is limited since the induced current loops have to be closed within the boundaries of the head, resulting in relatively strong return currents in posterior brain regions, away from the intended stimulation target. Similarly, when the C-core coil is positioned to straddle the forehead or vertex, it induces a circular electric field pattern in the sagittal plane of the head, with strongest field along the midline under the center of the coil. The return current path, however, passes through the base of the brain, which may result in undesired brainstem stimulation (see Figure 2(g)).

Sufficiently intense, high frequency, synchronous stimulation of various brain regions could trigger adverse acute or cumulative neuromodulation effects, including accidental seizure. If we assume that neural stimulation were an all-or-none event hinging on whether the electric field strength is below or above a neural activation threshold, then the most relevant parameter for evaluating the safety of dTMS would be the activated volume, V_A. In such case, smaller, more focal coils would be better for dTMS since they produce stronger superficial electric field but lower V_A than larger coils. On the other hand, if the severity of side effects depended on the absolute strength of the electric field or on the degree to which it exceeds the threshold for neural activation, a more relevant safety parameter would be the peak electric field strength in the cortex, max($|E_{2\ cm}|$). In that case, larger coils would be preferable since they reduce the superficial electric field magnitude at the expense of increased V_A.

Unfortunately, the respective contributions to risk of the peak electric field and the stimulated volume cannot be disentangled definitively from available data. For example, for

NIH-PA Author Manuscript

NIH-PA Author Manuscript

NIH-PA Author Manuscript

a given coil, raising the TMS pulse amplitude heightens the risk of a seizure (Wassermann, 1998; Rossi et al., 2009), but increasing pulse amplitude is associated with increases in both the peak electric field and the stimulated volume. Several cases of accidental seizure induction with H coils have been reported (Harel et al., 2011; Isserles et al., 2011; Levkovitz et al., 2011b,a; Isserles et al., 2013). In the H coil studies, the stimulation intensity was adjusted relative to motor threshold suggesting that the broader stimulated volume rather than the peak superficial electric field strength is contributing to increased risk of seizures. These studies, however, used different stimulation frequencies than studies with figure-8 coils, which may also affect seizure threshold (Wassermann, 1998; Peterchev et al., 2010). Finally, studies of magnetic seizure therapy have shown that coils with different field spatial profiles and placements have differential efficiency in inducing seizures (Lisanby et al., 2003; Deng et al., 2011), but these results are partially confounded by differences in the stimulus parameters such as the train frequency as well.

Another factor contributing to tolerability is the degree of scalp nerve and muscle activation. In order to reach a 6 cm deep target with threshold electric field strength, the scalp is stimulated at approximately 5 times threshold for the crown and C-core coils and 10–20 times threshold (data not shown) for the conventional figure-8, circular, and double cone coils. This may result in massive scalp muscle activation, which can lead to local pain and headache.

It should be noted that present safety guidelines for the use of TMS in clinical practice and research are based on data obtained with 70 mm figure-8 coils (Wassermann, 1998; Rossi et al., 2009), and may consequently not apply to dTMS coils with significantly deeper penetrating and broader electric field distributions. Therefore, safety should be evaluated for any novel dTMS coils and associated stimulation paradigms.

In conclusion, despite uncertainty about the risk factors for stimulation with nonfocal, deeply-penetrating electric fields, our results shown in Figures 3, 4, and 6 suggest that direct TMS of targets at depths of ~ 4 cm or more results in stimulation strength in superficial cortex that exceeds the upper limit in current rTMS safety guidelines. Approaching depths of ~ 6 cm is almost certainly unsafe considering the excessive superficial stimulation strength and activated brain volume.

4.3. Energy efficiency

A technical disadvantage of smaller coils is that they require more energy for stimulation. While the lower energy efficiency can be compensated by delivering more energy to the coil, this can present a challenge due to the increased power requirements, coil heating, internal coil forces, and noise. Full capacitor discharge of the Magstim 200, a low-frequency device, and the Magstim Rapid, a high-frequency rTMS device, can deliver a maximum of 725 J and 250 J, respectively (Hovey and Jalinous, 2006; Peterchev et al., 2008). Assuming pulse energy of 725 J, all coils in Figure 6(c) can stimulate targets at 4 cm; however, only the crown, double cone, and C-core coils can reach 6 cm targets. At 250 J, all coils except the figure-8 coil can stimulate targets at 4 cm, but only the crown coil can reach 6 cm targets. The conventional double cone coil is the most focal of the evaluated coils that can stimulate deep targets within the energy limit of standard TMS devices, and may therefore

NIH-PA Author Manuscript

NIH-PA Author Manuscript

NIH-PA Author Manuscript

represent a suitable choice for some dTMS studies. Distancing winding segments from the head, as in the H1 coil, results in decoupling of magnetic flux from the head, which increases the required stimulation energy.

The C-core coil size corresponding to minimum stimulation energy depends on the target depth (see Supplementary Figure S2). This observation could be helpful for selecting coil dimensions for brain targets at a specific depth. The C-core coil generates a figure-8-shaped electric field and has depth–focality ratio commensurate with figure-8 coils (Deng et al., 2013); however, it is unclear whether the optimal coil size behavior is generalizable to other figure-8 type coil topologies.

The coil energy requirements can be reduced in some cases by the use of ferromagnetic cores, as illustrated by the three-fold increase in efficiency of the ferromagnetic versus air core figure-8 coil. Moderate core saturation can be tolerated since the peak electric field strength is reached during the portion of the conventional sinusoidal stimulus waveform where current is changing most rapidly but has a small value (Epstein and Davey, 2002). However, substantial saturation reduces the coil output due to increase in the coil magnetic reluctance, and causes a sharp rise of the required coil current and energy, which loads the coil driving circuit. Therefore, the use of ferromagnetic cores may be impractical in some dTMS designs. In conclusion, the large energy required for stimulation of deep brain regions poses challenges that add to the safety concerns for reaching targets beyond ~ 4 cm.

4.4. Limitations

The results in this paper are from simulations in a spherical head model with homogeneous, isotropic conductivity. When dTMS coil designs are optimized for targeting specific brain regions, the head anatomy should be taken into account by simulating the electric field in realistic head models (e.g., (Thielscher et al., 2011)).

Another limitation to our model is the use of a single electric field threshold (1 V cm^{-1}) for neural activation throughout the brain. This value was derived in the literature from empirically determined motor thresholds coupled with simplified computational models or phantom measurements of the electric field (Epstein et al., 1990; Rudiak and Marg, 1994; Thielscher and Kammer, 2002; Komssi et al., 2007; Danner et al., 2012), and thus has accuracy limitations. We did not consider the electric field direction, which is known to affect the neural activation threshold (Di Lazzaro et al., 2001; Kammer et al., 2001; Balslev et al., 2007). However, dTMS affects wide regions of the brain which could contribute to partial averaging out of the effects of threshold variability among neural populations and electric field directions. Furthermore, the relative performance comparisons among different coils remain valid. Despite these limitations, we believe that comparing the performance of various coil configurations with a fixed neural activation threshold provides a useful set of characterizations that can inform coil design, safety analysis, interpretation of existing dTMS studies, and dose selection for planned dTMS studies.

This study did not evaluate all coils that produce deeply penetrating electric field. For example, the Magstim cap coil and the MagVenture twin coil have been used in MST studies (Deng et al., 2011; Kayser et al., 2011) and are particularly efficient for seizure

NIH-PA Author Manuscript

NIH-PA Author Manuscript

NIH-PA Author Manuscript

induction. Their efficiency is likely due to the more deeply penetrating and nonfocal electric field compared to the 90 mm circular coil and the double cone coil, respectively (Deng et al., 2011, 2013). Furthermore, as discussed in section 1, a variety of H coil designs intended for deep brain stimulation have been used in clinical studies. Nevertheless, H coils also follow the field depth–focality tradeoff represented by the range of coils in this study (Deng et al., 2013). Therefore, we expect the general conclusions of this paper to hold for other coil designs as well.

5. Conclusions

In this study, we compared the electric field characteristics of various dTMS coil designs. Both small and large TMS coils could, in principle, stimulate deep brain targets, provided that the energy is sufficient, and as long as the targets are not near the center of the head where the electric field is near zero. In the limiting case as the coil dimensions become large relative to the head, the electric field decay in depth becomes linear which is the slowest possible decay. The linear electric field attenuation limit allows us to estimate the maximum possible depth of direct neural activation at various stimulation intensities. Although smaller coils have a focality advantage over larger coils in terms of activated brain volume, this advantage diminishes with increasing target depth. Smaller coils also have the disadvantage of producing higher field strength in the superficial cortex and require more energy compared to larger coils. Collectively, these observations support the use of larger coils for dTMS. Although the electric field intensity of dTMS is within safety limits for tissue damage, there remain significant risks associated with strong and broad stimulation of superficial brain regions, including seizure. Existing safety guidelines may not apply to stimulation with the nonfocal and deeply penetrating electric fields occurring in dTMS. Nevertheless, our results indicate that direct TMS of targets at depths of ~ 4 cm or more results in superficial stimulation strength that exceeds the upper limit in current rTMS safety guidelines. Approaching depths of ~ 6 cm is almost certainly unsafe considering the excessive superficial stimulation strength and activated brain volume, and is technologically challenging as well. dTMS requires relatively high energy compared to superficial stimulation. While ferromagnetic cores improve electrical efficiency for targeting superficial brain areas, magnetic saturation reduces the effectiveness of the core for deeper targets, especially for highly focal coils. Distancing coil winding segments from the head, as in the H1 coil, increases the required stimulation energy. For C-core coils, there appears to be optimal coil size for minimum stimulation energy that depends on the target depth. In designing dTMS paradigms, all of these tradeoffs and limitations have to be considered, in addition to the specific affected non-target brains regions and subject discomfort resulting from scalp nerve and muscle stimulation. Of the standard commercial coils, the double cone coil offers high energy efficiency and a balance between stimulated volume and superficial field strength, making it suitable for some dTMS studies.

Supplementary Material

Refer to Web version on PubMed Central for supplementary material.

NIH-PA Author Manuscript

NIH-PA Author Manuscript

NIH-PA Author Manuscript

Acknowledgments

This work was supported in part by Faculty Development Award C040071 from the New York State Office of Science, Technology and Academic Research. Dr. Deng, Dr. Lisanby, and Dr. Peterchev are inventors on a patent application related to dTMS coils discussed in this paper and on other TMS technology patents and patent applications. Dr. Lisanby has served as Principal Investigator on industry-sponsored research grants to Columbia/RFMH or Duke (Neuronetics (past), Brainsway, ANS/St. Jude Medical, Cyberonics (past)); equipment loans to Columbia or Duke (Magstim, MagVenture); is supported by grants from NIH (R01MH091083, U01MH084241, R01MH060884), Stanley Medical Research Institute, National Alliance for Research on Schizophrenia and Depression, and the Wallace H. Coulter Foundation; and has no consultancies, speakers bureau memberships, board affiliations, or equity holdings in related industries. Dr. Peterchev served as Principal Investigator on a TMS research grant to Duke from Rogue Research and equipment donations to Columbia and Duke (Magstim, MagVenture); has received patent royalties from Rogue Research through Columbia for TMS technology unrelated to this manuscript; and is supported by NIH grants R01MH091083 and R21NS078687.

References

Agnew WF, McCreery DB. Considerations for safety in the use of extracranial stimulation for motor evoked potentials. Neurosurgery. 1987; 20:143–147. [PubMed: 3808255]

Al-Mutawaly N, de Bruin H, Findlay RD. Magnetic nerve stimulation: field focality and depth of penetration. Conf Proc IEEE Eng Med Biol Soc. 2001; ume 1:877–880.

Balslev D, Braet W, McAllister C, Miall RC. Inter-individual variability in optimal current direction for transcranial magnetic stimulation of the motor cortex. J Neurosci Methods. 2007; 162:309–313. [PubMed: 17353054]

Bersani FS, Girardi N, Sanna L, Mazzarini L, Santucci C, Kotzalidis GD, et al. Deep transcranial magnetic stimulation for treatment-resistant bipolar depression: a case report of acute and maintenance efficacy. Neurocase. 2012 In press:doi:10.1080/13554794.2012.690429.

Bersani FS, Minichino A, Enticott PG, Mazzarini L, Khan N, Antonacci G, et al. Deep transcranial magnetic stimulation as a treatment for psychiatric disorders: a comprehensive review. Eur Psychiatry. 2013; 28:30–39. [PubMed: 22559998]

Bewernick BH, Hurlemann R, Matusch A, Kayser S, Grubert C, Hadrysiewicz B, et al. Nucleus accumbens deep brain stimulation decreases ratings of depression and anxiety in treatment-resistant depression. Biol Psychiatry. 2010; 67:110–116. [PubMed: 19914605]

Carlezon WAJ, Rohan ML, Mague SD, Meloni EG, Parsegian A, Cayetano K, et al. Antidepressant-like effects of cranial stimulation within a low-energy magnetic field in rats. Biol Psychiatry. 2005; 57:571–576. [PubMed: 15780843]

Cohen D, Cuffin BN. Developing a more focal magnetic stimulator. Part I: Some basic principles. J Clin Neurophysiol. 1991; 8:102–111.

Crowther LJ, Marketos P, Williams PI, Melikhov Y, Jiles DC, Starzewski JH. Transcranial magnetic stimulation: improved coil design for deep brain investigation. J Appl Phys. 2011; 109:07B314.

Dalla, Libera D.; Colombo, B.; Coppi, E.; Straffi, L.; Chieffo, R.; Spagnolo, F., et al. Effects of high-frequency repetitive transcranial magnetic stimulation (rTMS) applied with H-coil for chronic migraine prophylaxis. Clin Neurophysiol. 2011; 122:S145–S146.

Danner N, Könönen M, Säisänen L, Laitinen R, Mervaala E, Julkunen P. Effect of individual anatomy on resting motor threshold—computed electric field as a measure of cortical excitability. J Neurosci Methods. 2012; 203:298–304. [PubMed: 22019330]

Davey, KR. The Oxford Handbook of Transcranial Stimulation. Oxford University Press; New York:

Davey KR, Epstein CM. Magnetic stimulation coil and circuit design. IEEE Trans Biomed Eng. 2000; 47:1439–1499.

Davey KR, Epstein CM, George MS, Bohning DE. Modeling the effects of electrical conductivity of the head on the induced electric field in the brain during magnetic stimulation. Clin Neurophysiol. 2003; 114:2204–2209. [PubMed: 14580620]

Davey KR, Riehl ME. Suppressing the surface field during transcranial magnetic stimulation. IEEE Trans Biomed Eng. 2006; 53:190–194. [PubMed: 16485747]

NIH-PA Author Manuscript

NIH-PA Author Manuscript

NIH-PA Author Manuscript

Deng ZD, Lisanby SH, Peterchev AV. Electric field strength and focality in electroconvulsive therapy and magnetic seizure therapy: a finite element simulation study. J Neural Eng. 2011; 8:016007. [PubMed: 21248385]

Deng ZD, Lisanby SH, Peterchev AV. Electric field depth–focality tradeoff in transcranial magnetic stimulation: simulation comparison of 50 coil designs. Brain Stimul. 2013; 6:1–13. [PubMed: 22483681]

Deng ZD, Peterchev AV, Lisanby SH. Coil design considerations for deep-brain transcranial magnetic stimulation (dTMS). Conf Proc IEEE Eng Med Biol Soc. 2008:5675–5679. [PubMed: 19164005]

Di Lazzaro V, Oliviero A, Mazzone P, Insola A, Pilato F, Saturno E, et al. Comparison of descending volleys evoked by monophasic and biphasic magnetic stimulation of the motor cortex in conscious humans. Exp Brain Res. 2001; 141:121–127. [PubMed: 11685416]

Downar J, Daskalakis ZJ. New targets for rTMS in depression: a review of convergent evidence. Brain Stimul. 2013; 6:231–40. [PubMed: 22975030]

Eaton H. Electric field induced in a spherical volume conductor from arbitrary coils: application to magnetic stimulation and MEG. Med Biol Eng Comput. 1992; 30:433–440. [PubMed: 1487945]

Enticott PG, Kennedy HA, Zangen A, Fitzgerald PB. Deep repetitive transcranial magnetic stimlation associated with improved social functioning in a young woman with an autism spectrum disorder. J ECT. 2011; 27:41–43. [PubMed: 20966773]

Epstein CM, Davey KR. Iron-core coils for transcranial magnetic stimulation. J Clin Neurophysiol. 2002; 19:376–381. [PubMed: 12436092]

Epstein CM, Schwartzberg DG, Davey KR, Sudderth DB. Localizing the site of magnetic brain stimulation in humans. Neurology. 1990; 40:666–670. [PubMed: 2320243]

Fitzgerald PB, Daskalakis ZJ. The effects of repetitive transcranial magnetic stimulation in the treatment of depression. Expert Rev Med Devices. 2011; 8:85–95. [PubMed: 21158543]

Fitzgerald PB, Fountain S, Daskalakis ZJ. A comprehensive review of the effects of rTMS on motor cortical excitability and inhibition. Clin Neurophysiol. 2006; 117:2584–2596. [PubMed: 16890483]

Grandori F, Ravazzani P. Magnetic stimulation of the motor cortex—theoretical considerations. IEEE Trans Biomed Eng. 1991; 38:180–191. [PubMed: 2066128]

Greenberg BD, Friehs GM, Carpenter L, Tyrka A, Malone DA, Rezai AR, et al. Deep brain stimulation: clinical findings in intractable depression and OCD. Neuropsychopharm. 2005; 29:S32.

Harel EV, Rabany L, Deutsch L, Bloch Y, Zangen A, Levkovitz Y. H-coil repetitive transcranial magnetic stimulation for treatment resistant major depressive disorder: an 18-week continuation safety and feasibility study. World J Biol Psychiatry. 2012 In press:doi: 10.3109/15622975.2011.639802.

Harel EV, Zangen A, Roth Y, Reti I, Braw Y, Levkovitz Y. H-coil repetitive transcranial magnetic stimulation for the treatment of bipolar depression: an add-on, safety and feasibility study. World J Biol Psychiatry. 2011; 12:119–126. [PubMed: 20854181]

Haus, HA.; Melcher, JR. Electromagnetic Fields and Energy. Printice-Hall; New Jersey: 1989.

Hayward G, Mehta MA, Harmer C, Spinks TJ, Grasby PM, Goodwin GM. Exploring the physiological effects of double-cone coil TMS over the medial frontal cortex on the anterior cingulate cortex: an H215O PET study. Eur J Neurosci. 2007; 25:2224–2233. [PubMed: 17439499]

Heller L, van Hulsteyn DB. Brain stimulation using electromagnetic sources: theoretical aspects. Biophys J. 1992; 63:129–138. [PubMed: 1420862]

Holtzheimer PE, Kelley ME, Gross RE, Filkowski MM, Garlow SJ, Barrocas A, et al. Subcallosal cingulate deep brain stimulation for treatment-resistant unipolar and bipolar depression. Arch Gen Psychiatry. 2012; 69:150–158. [PubMed: 22213770]

Hovey, C.; Jalinous, R. [Last accessed Nov. 17, 2011] The guide to magnetic stimulation. 2006. http://www.icts.uci.edu/neuroimaging/GuidetoMagneticStimulation2008.pdf

IEEE Std C95.1-2005. IEEE standard for safety levels with respect to human exposure to radio frequency electromagnetic fields, 3 kHz to 300 GHz. 2005

NIH-PA Author Manuscript

NIH-PA Author Manuscript

NIH-PA Author Manuscript

International Commission on Non-Ionizing Radiation Protection. Guidelines for limiting exposure to time-varying electric and magnetic fields (1 Hz to 100 kHz). Health Phys. 2010; 99:818–836. [PubMed: 21068601]

Ishii K, Matsuzaka Y, Izumi S, Abe T, Nakazato N, Okita T, et al. Evoked motor response following deep transcranial magnetic stimulation in a cynomolgus monkey. Brain Stimul. 2008; 1:300.

Isserles M, Rosenberg O, Dannon P, Levkovitz Y, Kotler M, Deutsch F, et al. Cognitive-emotional reactivation during deep transcranial magnetic stimulation over the prefrontal cortex of depressive patients affects antidepressant outcome. J Affect Disord. 2011; 128:235–342. [PubMed: 20663568]

Isserles M, Shalev AY, Roth Y, Peri T, Kutz I, Zlotnick E, et al. Effectiveness of deep transcranial magnetic stimulation combined with a brief exposure procedure in post-traumatic stress disorder—a pilot study. Brain Stimul. 2013; 6:377–83. [PubMed: 22921765]

Jackson, JD. Classical Electrodynamics. 3rd ed. John Wiley & Sons, Inc.; New York: 1999.

Jiménez F, Velasco F, Salin-Pascual R, Hernández JA, Velasco M, Criales JL, et al. A patient with a resistant major depression disorder treated with deep brain stimulation in the inferior thalamic peduncle. Neurosurgery. 2005; 57:585–593. [PubMed: 16145540]

Johansen-Berg H, Gutman DA, Behrens TEJ, Matthews PM, Rushworth MFS, Katz E, et al. Anatomical connectivity of the subgenual cingulate region targeted with deep brain stimulation for treatment-resistant depression. Cereb Cortex. 2008; 18:1374–1383. [PubMed: 17928332]

Johnson KA, Baig M, Ramsey D, Lisanby SH, Avery D, McDonald WM, et al. Prefrontal rTMS for treating depression: location and intensity results from the OPT-TMS multi-site clinical trial. Brain Stimul. 2013; 2:108–17. [PubMed: 22465743]

Kammer T, Beck S, Thielscher A, Laubis-Hermann U, Topka H. Motor thresholds in humans: a transcranial magnetic stimulation study comparing different pulse waveforms, current directions and stimulator types. Clin Neurophysiol. 2001; 112:250–258. [PubMed: 11165526]

Kayser S, Bewernick BH, Grubert C, Hadrysiewicz BL, Axmacher N, Schlaepfer TE. Antidepressant effects, of magnetic seizure therapy and electroconvulsive therapy, in treatment-resistant depression. J Psychiatr Res. 2011; 45:569–576. [PubMed: 20951997]

Kennedy SH, Giacobbe P, Rizvi SJ, Placenza FM, Nishikawa Y, Mayberg HS, et al. Deep brain stimulation for treatment-resistant depression: follow-up after 3 to 6 years. Am J Psychiatry. 2011; 168:502–510. [PubMed: 21285143]

Komssi S, Savolainen P, Heiskala J, Kähkönen S. Excitation threshold of the motor cortex estimated with transcranial magnetic stimulation electroencephalography. Neuroreport. 2007; 18:13–16. [PubMed: 17259853]

Kranz G, Shamim EA, Lin PT, Kranz GS, Hallett M. Transcranial magnetic brain stimulation modulates blepharospasm: a randomized controlled study. Neurology. 2010; 75:1465–1471. [PubMed: 20956792]

Krause L, Enticott PG, Zangen A, Fitzgerald PB. The role of medial pre-frontal cortex in theory of mind: a deep rTMS study. Behav Brain Res. 2012; 228:87–90. [PubMed: 22155478]

Levkovitz Y, Harel EV, Roth Y, Braw Y, Most D, Katz LN, et al. Deep transcranial magnetic stimulation over the prefrontal cortex: evaluation of antidepressant and cognitive effects in depressive patients. Brain Stimul. 2009; 2:188–200. [PubMed: 20633419]

Levkovitz Y, Rabany L, Harel EV, Zangen A. Deep transcranial magnetic stimulation add-on for treatment of negative symptoms and cognitive deficits of schizophrenia: a feasibility study. Int J Neuropsychopharmacol. 2011a; 12:991–996. [PubMed: 21524336]

Levkovitz Y, Roth Y, Harel EV, Braw Y, Sheer A, Zangen A. A randomized controlled feasibility and safety study of deep transcranial magnetic stimulation. Clin Neurophysiol. 2007; 118:2730–2744. [PubMed: 17977787]

Levkovitz Y, Sheer A, Harel EV, Katz LN, Most D, Zangen A, et al. Differential effects of deep TMS of the prefrontal cortex on apathy and depression. Brain Stimul. 2011b; 4:266–274. [PubMed: 22032742]

Lisanby SH, Luber B, Schlaepfer TE, Sackeim HA. Safety and feasibility of magnetic seizure therapy (MST) in major depression: randomized within-subject comparison with electroconvulsive therapy. Neuropsychopharmacology. 2003; 28:1852–1865. [PubMed: 12865903]

NIH-PA Author Manuscript

NIH-PA Author Manuscript

NIH-PA Author Manuscript

Lisanby SH, Schlaepfer TE, Fisch HU, Sackeim HA. Magnetic seizure therapy of major depression. Arch Gen Psychiatry. 2001; 58:303–305. [PubMed: 11231838]

Logothetis NK, Kayser C, Oeltermann A. *In vivo* measurement of cortical impedance spectrum in monkeys: implications for signal propagation. Neuron. 2007; 55:809–823. [PubMed: 17785187]

Lontis ER, Voigt M, Struijk JJ. Focality assessment in transcranial magnetic stimulation with double and cone coils. J Clin Neurophysiol. 2006; 23:463–472.

Lozano AM, Mayberg HS, Giacobbe P, Hamani C, Craddock RC, Kennedy SH. Subcallosal cingulate gyrus deep brain stimulation for treatment-resistant depression. Biol Psychiatry. 2008; 64:461–467. [PubMed: 18639234]

Malone DAJ, Dougherty DD, Rezai AR, Carpenter LL, Friehs GM, Eskandar EN, et al. Deep brain stimulation of the ventral capsule/ventral striatum for treatment-resistant depression. Biol Psychiatry. 2009; 65:267–275. [PubMed: 18842257]

Mayberg HS, Lozano AM, Voon V, McNeely HE, Seminowicz DA, Hamani C, et al. Deep brain stimulation for treatment-resistant depression. Neuron. 2005; 45:651–660. [PubMed: 15748841]

Miranda PC, Correia L, Salvador R, Basser PJ. Tissue heterogeneity as a mechanism for localized neural stimulation by applied electric fields. Phys Med Biol. 2007; 52:5603–5617. [PubMed: 17804884]

Miranda PC, Hallett M, Basser PJ. The electric field induced in the brain by magnetic stimulation: a 3-D finite-element analysis of the effect of tissue heterogeneity and anisotropy. IEEE Trans Biomed Eng. 2003; 50:1074–1085. [PubMed: 12943275]

Opitz A, Windhoff M, Heidemann RM, Turner R, Thielscher A. How the brain tissue shapes the electric field induced by transcranial magnetic stimulation. NeuroImage. 2011; 58:849–859. [PubMed: 21749927]

Peterchev, AV.; Chan, B.; Lisanby, SH. Optimal frequency for seizure induction. 20th Annual Meeting of the International Society for Neurostimulation; J ECT. 2010. p. 154

Peterchev AV, Jalinous R, Lisanby SH. A transcranial magnetic stimulator inducing near-rectangular pulses with controllable pulse width (cTMS). IEEE Trans Biomed Eng. 2008; 55:257–266. [PubMed: 18232369]

Peterchev AV, Murphy DL, Lisanby SH. Repetitive transcranial magnetic stimulator with controllable pulse parameters. J Neural Eng. 2011; 8:036016. [PubMed: 21540487]

Peterchev AV, Wagner TA, Miranda PC, Nitsche MA, Paulus W, Lisanby SH, et al. Fundamentals of transcranial electric and magnetic stimulation dose: definition, selection, and reporting practices. Brain Stimul. 2012; 5:435–453. [PubMed: 22305345]

Plonsey R, Heppner D. Considerations of quasi-stationarity in electrophysiological systems. Bulletin of Mathematical Biophysics. 1967; 29:657–664. [PubMed: 5582145]

Ravazzani P, Ruohonen J, Grandori F, Tognola G. Magnetic stimulation of the nervous system: induced electric field in unbounded, semi-infinite, spherical, and cylindrical media. Ann Biomed Eng. 1996; 24:606–616. [PubMed: 8886241]

Rohan M, Parow A, Stoll AL, Demopulos C, Friedman S, Dager S, et al. Low-field magnetic stimulation in bipolar depression using an MRI-based stimulator. Am J Psychiatry. 2004; 161:93–98. [PubMed: 14702256]

Rosenberg O, Isserles M, Levkovitz Y, Kotler M, Zangen A, Dannon PN. Effectiveness of a second deep TMS in depression: a brief report. Prog Neuropsychopharmacol Biol Psychiatry. 2011a; 35:1041–1044. [PubMed: 21354242]

Rosenberg O, Roth Y, Kotler M, Zangen A, Dannon P. Deep transcranial magnetic stimulation for the treatment of auditory hallucinations: a preliminary open-label study. Ann Gen Psychiatry. 2011b; 10:3. [PubMed: 21303566]

Rosenberg O, Shoenfeld N, Zangen A, Kotler M, Dannon PN. Deep TMS in a resistant major depressive disorder: a brief report. Depress Anxiety. 2010a; 27:465–469. [PubMed: 20455247]

Rosenberg O, Zangen A, Stryjer R, Kotler M, Dannon PN. Response to deep TMS in depressive patients with previous electroconvulsive treatment. Brain Stimul. 2010b; 3:211–217. [PubMed: 20965450]

NIH-PA Author Manuscript

NIH-PA Author Manuscript

NIH-PA Author Manuscript

Rösler KM, Hess CW, Heckmann R, Ludin HP. Significance of shape and size of the stimulating coil in magnetic stimulation of the human motor cortex. Neurosci Lett. 1989; 100:347–352. [PubMed: 2761784]

Rossi S, Hallett M, Rossini PM, Pascual-Leone A, Safety of TMS Consensus Group. Safety, ethical considerations, and application guidelines for the use of transcranial magnetic stimulation in clinical practice and research. Clin Neurophysiol. 2009; 120:2008–2039. [PubMed: 19833552]

Roth BJ, Cohen LG, Hallett M, Friauf W, Basser PJ. A theoretical calculation of the electric field induced by magnetic stimulation of a peripheral nerve. Muscle Nerve. 1990; 13:734–741. [PubMed: 2385260]

Roth BJ, Saypol JM, Hallett M, Cohen LG. A theoretical calculation of the electric field induced in the cortex during magnetic stimulation. Electroencephalogr Clin Neurophysiol. 1991; 81:47–56. [PubMed: 1705219]

Roth Y, Amir A, Levkovitz Y, Zangen A. Three-dimensional distribution of the electric field induced in the brain by transcranial magnetic stimulation using figure-8 and deep H-coils. J Clin Neurophysiol. 2007a; 24:31–38. [PubMed: 17277575]

Roth, Y.; Padberg, F.; Zangen, A. Transcranial Brain Stimulation for Treatment of Psychiatric Disorders. Karger; Basel: 2007.

Roth Y, Pell GS, Zangen A. Commentary on: Deng et al., Electric field depth-focality tradeoff in transcranial magnetic stimulation: simulation comparison of 50 coil designs. Brain Stimul. 2013; 6:14–15. [PubMed: 22560047]

Roth, Y.; Zangen, A. Transcranial magnetic stimulation of deep brain regions. 3rd ed. CRC Press/ Taylor & Francis; Boca Raton, FL.: 2006.

Roth Y, Zangen A, Hallett M. A coil design for transcranial magnetic stimulation of deep brain regions. J Clin Neurophysiol. 2002; 19:361–370. [PubMed: 12436090]

Rudiak D, Marg E. Finding the depth of magnetic brain stimulation: a re-evaluation. Electroenceph Clin Neurophysiol. 1994; 93:358–371. [PubMed: 7525244]

Ruohonen, J.; Ilmoniemi, RJ. Handbook of Transcranial Magnetic Stimulation. Oxford University Press; New York: 2002. p. 18-30.

Salvador R, Miranda PC, Roth Y, Zangen A. High-permeability core coils for transcranial magnetic stimulation of deep brain regions. Conf Proc IEEE Eng Med Biol Soc. 2007:6652–6655.

Salvador R, Miranda PC, Roth Y, Zangen A. High permeability cores to optimize the stimulation of deeply located brain regions using transcranial magnetic stimulation. Phys Med Biol. 2009; 54:3113–3128. [PubMed: 19420425]

Sartorius A, Henn FA. Deep brain stimulation of the lateral habenula in treatment resistant major depression. Med Hypotheses. 2007; 69:1305–1308. [PubMed: 17498883]

Sartorius A, Kiening KL, Kirsch P, von Gall CC, Haberkorn U, Unterberg AW, et al. Remission of major depression under deep brain stimulation of the lateral habenula in a therapy-refractory patient. Biol Psychiatry. 2010; 67:e9–e11. [PubMed: 19846068]

Saypol JM, Roth BJ, Cohen LG, Hallett M. A theoretical comparison of electric and magnetic stimulation of the brain. Ann Biomed Eng. 1991; 19:317–328. [PubMed: 1928873]

Schlaepfer TE, Cohen MX, Frick C, Kosel M, Brodesser D, Axmacher N, et al. Deep brain stimulation to reward circuitry alleviates anhedonia in refractory major depression. Neuropsychopharm. 2008; 33:368–377.

Seminowicz DA, Mayberg HS, McIntosh AR, Goldapple K, Kennedy S, Segal Z, et al. Limbic-frontal circuitry in major depression: a path modeling metanalysis. NeuroImage. 2004; 22:409–418. [PubMed: 15110034]

Tartaglia G, Gabriele M, Frasca V, Pichiorri F, Giacomelli E, Cambieri C, et al. Pain relief by deep repetitive transcranial magnetic stimulation applied with the H-coil. Clin Neurophysiol. 2011; 122:S144.

Terao Y, Ugawa Y, Sakai K, Uesaka Y, Kohara N, Kanazawa I. Transcranial stimulation of the leg area of the motor cortex in humans. Acta Neurol Scand. 1994; 89:378–383. [PubMed: 8085437]

Thielscher A, Kammer T. Linking physics and physiology in TMS: a sphere field model to determine the cortical stimulation site in TMS. NeuroImage. 2002; 17:1117–1130. [PubMed: 12414254]

NIH-PA Author Manuscript

NIH-PA Author Manuscript

NIH-PA Author Manuscript

Thielscher A, Opitz A, Windhoff M. Impact of the gyral geometry on the electric field induced by transcranial magnetic stimulation. NeuroImage. 2011; 54:234–243. [PubMed: 20682353]

Trebbastoni A, Raccah R, de Lena C, Zangen A, Inghilleri M. Repetitive deep transcranial magnetic stimulation improves verbal fluency and written language in a patient with primary progressive aphasia-logopenic variant (LPPA). Brain Stim. 2012; 6:545–53.

Ueno S, Tashiro T, Harada K. Localized stimulation of neural tissues in the brain by means of a paired configuration of time-varying magnetic fields. J Appl Phys. 1988; 64:5862–5864.

Volkow ND, Tomasi D, Wang GJ, Fowler JS, Telang F, Wang R, et al. Effects of low-field magnetic stimulation on brain glucose metabolism. NeuroImage. 2010; 51:623–628. [PubMed: 20156571]

Wagner TA, Zahn M, Grodzinsky AJ, Pascual-Leone A. Three-dimensional head model simulation of transcranial magnetic stimulation. IEEE Trans Biomed Eng. 2004; 51:1586–1598. [PubMed: 15376507]

Wassermann EM. Risk and safety of repetitive transcranial magnetic stimulation: report and suggested guidelines from the International Workshop on the Safety of Repetitive Transcranial Magnetic Stimulation, June 5–7, 1996. Electroenceph Clin Neurophysiol. 1998; 108:1–16. [PubMed: 9474057]

Zangen A, Roth Y, Voller B, Hallett M. Transcranial magnetic stimulation of deep brain regions: evidence for efficacy of the H-coil. Clin Neurophysiol. 2005; 116:775–779. [PubMed: 15792886]

NIH-PA Author Manuscript

NIH-PA Author Manuscript

NIH-PA Author Manuscript

Highlights

- The focality advantage of smaller TMS coils over larger coils diminishes with increasing target depth.
- At best (for large TMS coils), the electric field attenuation in the brain relative to the head surface is directly proportional to the target depth.
- Direct rTMS of targets at depths of ~ 4 cm or more is likely unsafe as it results in superficial stimulation strength that exceeds the upper limit in current rTMS safety guidelines.

NIH-PA Author Manuscript

NIH-PA Author Manuscript

NIH-PA Author Manuscript

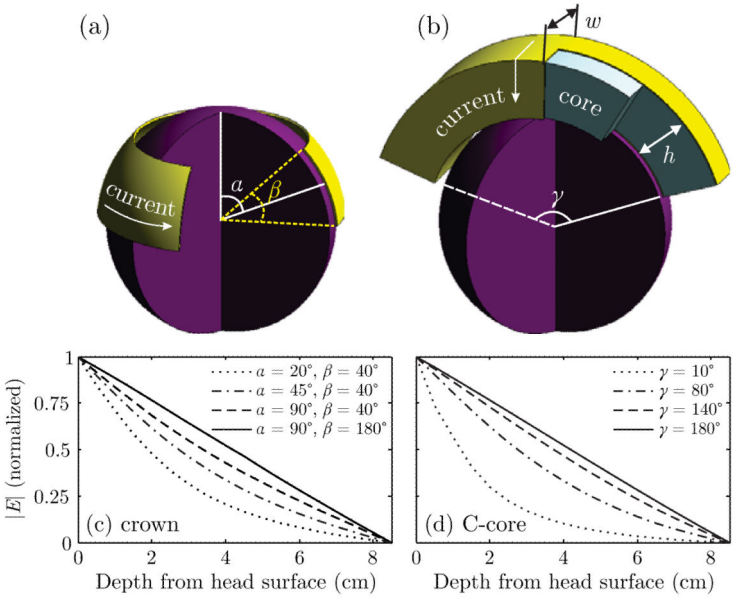

Figure 1.

Cutaway views of the (a) crown and (b) C-core coil models. The direction of coil current flow is indicated with arrows. Plots (c) and (d) show the electric field attenuation in depth relative to the field strength at the head surface of the crown coil and the C-core coil ($h = w = 7$ cm) for various opening angles. The spherical head model has radius of 8.5 cm.

NIH-PA Author Manuscript

NIH-PA Author Manuscript

NIH-PA Author Manuscript

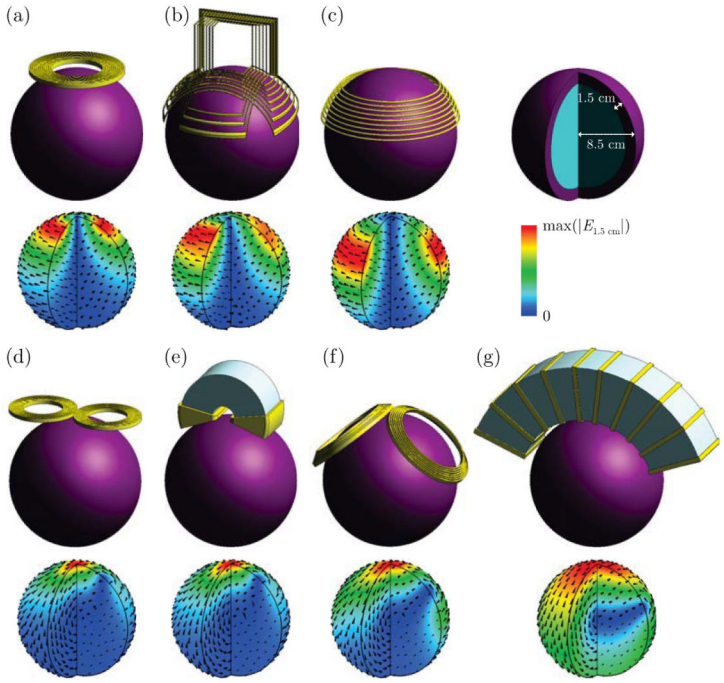

Figure 2.

Simulation models of seven TMS coil configurations and the corresponding electric field distribution in the brain: (a) Magstim 90 mm circular coil, (b) Brainsway H1 coil, (c) crown coil (α = 65°, β = 40°; Figure 1(a)), (d) Magstim 70 mm figure-8 coil, (e) Neuronetics iron core figure-8 coil, (f) Magstim double cone coil, (g) stretched C-core coil (γ = 140°, h = w = 7 cm; Figure 1(b)). A quarter of the brain sphere is removed to visualize the electric field in depth. The electric field magnitude is normalized to the peak electric field on the cortical surface, max(|$E_{1.5\ cm}$|).

NIH-PA Author Manuscript

NIH-PA Author Manuscript

NIH-PA Author Manuscript

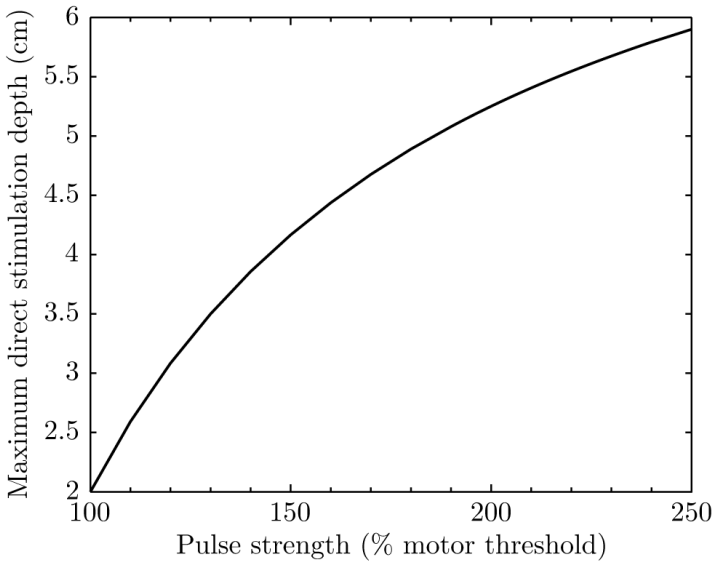

Figure 3.

Maximum direct stimulation depth versus stimulation strength in superficial cortex relative to motor threshold. The stimulation depth is estimated with equation (2) which assumes a large dTMS coil with linear electric field decay with distance, and thus represents the deepest possible direct stimulation for any coil. Note that in this extreme case the stimulation is also most nonfocal. The target area for conventional motor threshold determination is assumed to be at 2 cm depth.

NIH-PA Author Manuscript
NIH-PA Author Manuscript
NIH-PA Author Manuscript

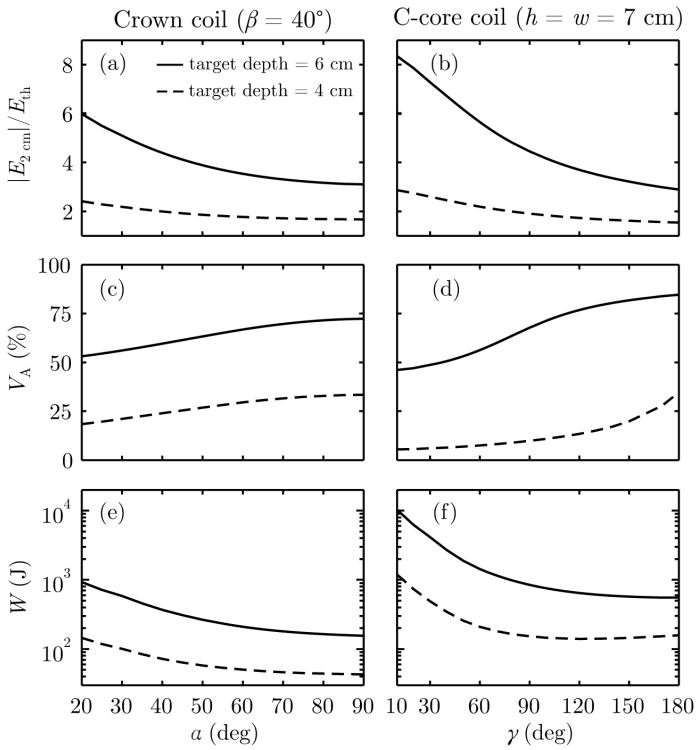

Figure 4.

Crown and C-core coil performance as a function of target depth (dashed line: 4 cm, solid line: 6 cm) and coil size parametrized by angles α and γ (see Figure 1 for angle definitions). Left column: angle β of the crown coil is fixed at 40° while α is varied from 20°–90°. Varying angle β in the crown coil while holding α fixed at 90° results in similar trends (see Supplementary Figure S1). Right column: γ of the C-core coil is varied from 10°–180°. Evaluated metrics are: (a–b) maximum electric field strength in the cortex relative to neural activation threshold, $\max(|E_{2\,\mathrm{cm}}|)/E_{\mathrm{th}}$, (c–d) directly activated brain volume, V_{A}, and (e–f) energy delivered to the coil assuming $E_{\mathrm{th}} = 1$ V cm^{-1}, W.

NIH-PA Author Manuscript
NIH-PA Author Manuscript
NIH-PA Author Manuscript

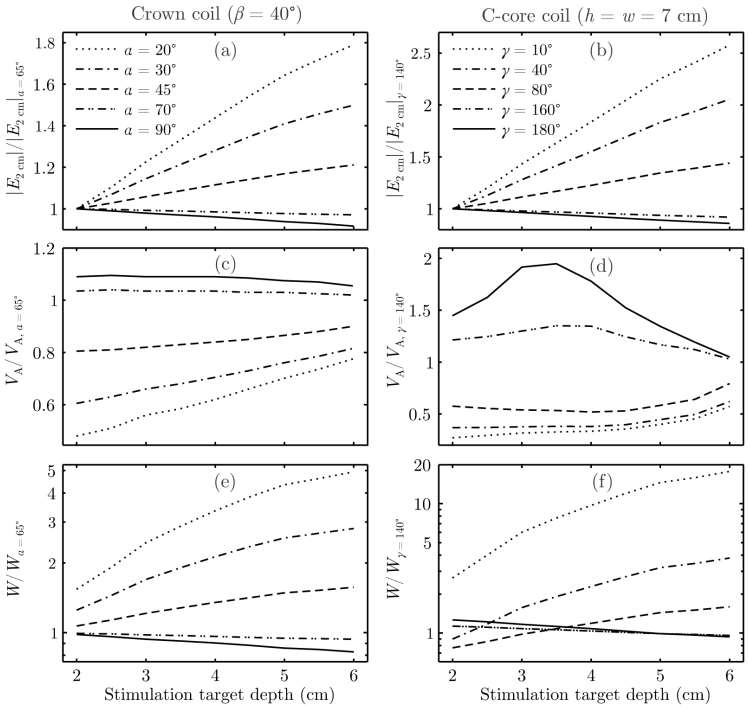

Figure 5.

Relative performance of crown (left column) and C-core (right column) coils of various sizes for stimulation of targets at depths of 2–6 cm: (a–b) maximum electric field strength in the superficial cortex, max(|$E_{2\,\mathrm{cm}}$|); (c–d) directly activated brain volume, V_A; and (e–f) energy delivered to the coil, W. The metrics are normalized to those of the nominal crown coil ($\alpha = 65°$, $\beta = 40°$) and C-core coil ($\gamma = 140°$, $h = w = 7$ cm) shown in Figure 2(c) and (g), respectively.

NIH-PA Author Manuscript
NIH-PA Author Manuscript
NIH-PA Author Manuscript

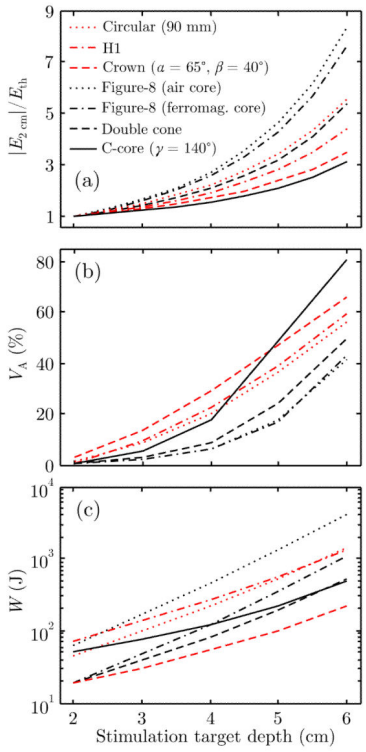

Figure 6.

Performance metrics of the seven TMS coil configurations shown in Figure 2 for stimulation target depths of 2–6 cm: (a) maximum electric field in the superficial cortex relative to neural activation threshold, max($|E_{2\,cm}|$)/E_{th}; (b) directly activated brain volume, V_A; and (c) energy delivered to the coil assuming E_{th} = 1 V cm^{-1}, W. The curves for coils with circular and double loop electric field patterns are shown in red and black, respectively.